Phase-only hologram generation based on integral imaging and its enhancement in depth resolution

Jiwoon Yeom[1], Jisoo Hong[1], Jae-Hyun Jung[1], Keehoon Hong[1], Jae-Hyeung Park[2], and Byoungho Lee[1]*

[1]*School of Electrical Engineering, Seoul National University, Gwanak-Gu Gwanakro 1, Seoul, 151-744, Korea*

[2]*School of Information and Communication Engineering, Chungbuk National University, 410 SungBong-Ro, Heungduk-Gu, Cheongju-Si, Chungbuk, 361-763, Korea*

**Corresponding author: byoungho@snu.ac.kr*

Received July 30, 2011; accepted September 27, 2011; posted online November 18, 2011

We introduce a phase-only hologram generation method based on an integral imaging, and propose an enhancement method in representable depth interval. The computational integral imaging reconstruction method is modified based on optical flow to obtain depth-slice images for the focused objects only. A phase-only hologram for multiple plane images is generated using the iterative Fresnel transform algorithm. In addition, a division method in hologram plane is proposed for enhancement in the representable minimum depth interval.

OCIS codes: 090.0090, 100.0100.
doi: 10.3788/COL201109.120009.

Three-dimensional (3D) display is one of the most attractive fields in display technologies, and various methods in processing 3D information have been widely studied[1]. Among them is holography, which has been thought as an ultimate method for describing 3D information since it is capable of reconstructing the whole wavefront of a recorded object wave. However, the recording process of holography requires complicated and bulky experimental setup, including coherent light sources. The requirement for a well-aligned optical system makes it hard to capture real objects outdoors.

Several researchers have adopted integral imaging (II) to overcome the requirements in the capture process of holography[2−4]. Since II provides a compact pickup process in which 3D information is captured under an incoherent light source, the high requirements of the traditional holography recording process can be alleviated. Many researchers verified the performance of hologram generated based on II using perspective view images or orthographic view images as the source of information.

In our previous research[4], we proposed a compact method for making the phase-only hologram of 3D objects using computational II reconstruction (CIIR) and iterative Fresnel transform algorithm (IFTA), as shown in Fig. 1. One of merits in this study is that the computer generated hologram (CGH) only has phase profile with constant amplitude distribution. Since phase-only modulation devices are widely used due to their efficiency, it is an important issue to make constant amplitude profile in the CGH. To satisfy the constant amplitude distribution, we used the modified IFTA for the multi-plane images[5].

In this letter, we verify the limitation of our previous work, and propose an enhancement method for generating hologram with higher depth resolution. The modified CIIR method for obtaining depth-slice images without blurred ones based on optical flow is discussed. In addition, space multiplexing in hologram plane is adopted to improve the representable depth interval. The simulation and experimental results are provided to verify the proposed method.

In the pickup process of II, 3D objects are captured through the lens array as a form of elemental image set. The elemental image set contains various perspective images, which are captured at different positions. From this property, the elemental image set is applied for other purposes such as depth map calculation[6,7], occluded region reconstruction[7], and depth-slice image generation[8,9]. We use the elemental image set for the purpose of generating depth-slice images, which is the basic information for multi-plane phase-only hologram[4].

The individual depth-slice image is placed at the proper

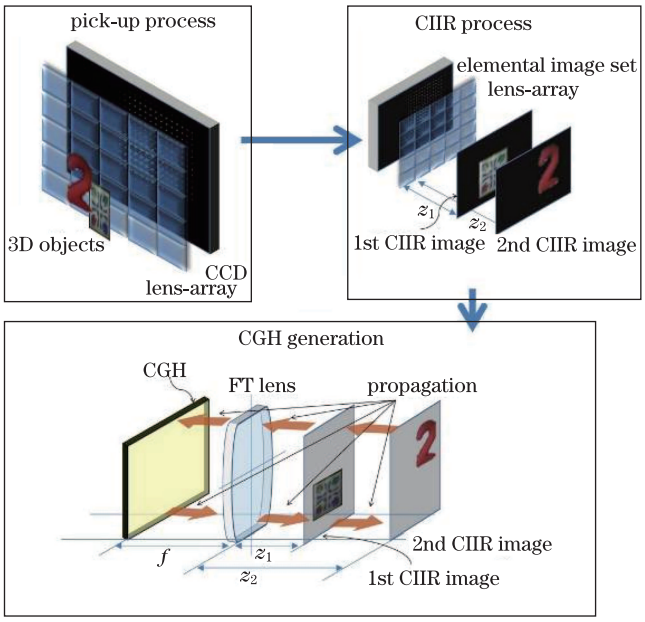

Fig. 1. Overall process of hologram generation based on II. FT: Fresnel transform.

depth plane and converted into phase-only hologram using IFTA for multiple planes[5]. In the IFTA, each target image is propagated into the next depth plane, and the phase distribution in the complex amplitude of the propagated wave is extracted to be combined with the new target image. During the process, propagation over distance z is performed using the Fresnel diffraction integral[10]. At the hologram plane, the constant amplitude condition is forced, and the phase profile of the hologram is propagated to image planes with inverse direction. This process is repeated until the CGH has almost constant amplitude.

The basic CIIR used in the previous hologram generation method is not suitable for generating exact depth-slice images because the unfocused object leads to blurred images. In general, the depth-slice image must contain only the information of the focused part in the object. However, images generated based on the basic CIIR method contain not only information on the focused objects, but also on the unfocused ones. To demonstrate an example of the basic CIIR method, we captured two objects that were located at a distance of 40 and 70 mm away from the lens array, as shown in Fig. 2(a). Figures 3(a) and (b) show the depth-slice images using the basic CIIR method based on the estimated depth map of Fig. 2(b). In the depth-slice image for the first object, Fig. 3(a), the blurred version of the second object image is shown and vice versa. These blurred images are one of the reasons for the image degradation of the reconstructed images of the hologram.

In addition, it is not possible to represent the correct target images in the CGH if the interval between adjacent depth planes is too small. Figure 4(a) shows the CGH, while Figs. 4(b) and (c) show the numerical reconstruction results with depth interval of 5 mm. The focal length of Fourier transform (FT) lens, f, is assumed to be 100 mm. We used CIIR images provided in Figs. 3(c) and (d), which are generated based on the modified CIIR method which is discussed later. Since our goal is to examine the effect of small depth interval on the reconstructed image quality, it is necessary to minimize the effect of the blurred images due to the unfocused objects with the modified CIIR method. As shown in Fig. 4(c), which is the reconstructed result of the second target image, ghost images of the first target image exist. In the same manner, some parts of the second target image are shown in Fig. 4(b). These ghost images are different from the blurred portion in the CIIR images, as shown in Figs. 3(a) and (b). They occur because the depth interval between two planes, Δz, is too small[5]. This problem becomes severe as the distance between the two depth planes becomes smaller. Although

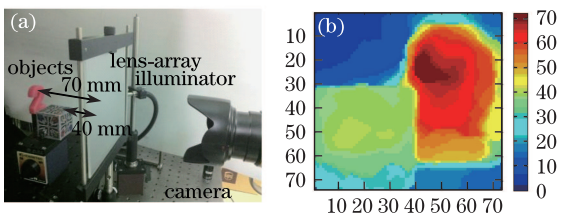

Fig. 2. Overall pickup process. (a) Experimental setup and (b) extracted depth map.

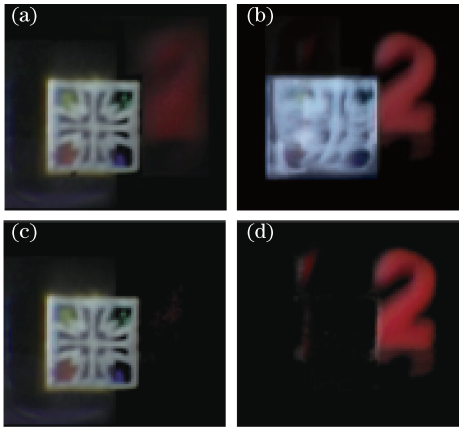

Fig. 3. CIIR images with basic CIIR method at (a) z_1= 40 mm and (b) z_2= 70 mm, and with modified CIIR method at (c) z_1= 40 mm and (d) z_2= 70 mm.

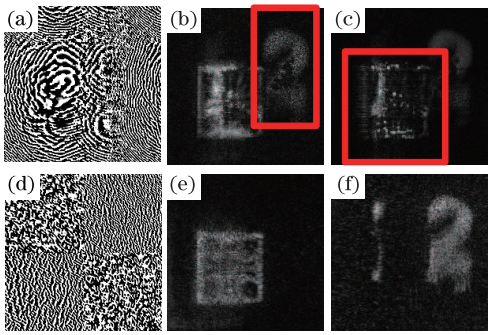

Fig. 4. Hologram generation process. (a) CGH without hologram division method and its numerically reconstructed images at (b) z_1= 40 mm and (c) z_2= 45 mm; (d) CGH with hologram division method and its numerically reconstructed images at (e) z_1= 40 mm and (f) z_2= 45 mm.

we eliminate the blurred parts due to the unfocused objects in the CIIR method, the overlapped images can still appear as the distance between adjacent planes becomes closer.

Figure 5(a) presents the peak signal-to-noise ratio (PSNR) values according to Δz when f is equal to 100, 150, and 200 mm. In the figure legend of Fig. 5(a), "case I" means the PSNR values in the case of undivided hologram, and "case II" refers to the PSNR values with the hologram division method. The PSNR values of the numerically reconstructed images with undivided hologram decrease as Δz is decreased, because the pixels of the hologram represent different information at each depth. The wave propagated from the hologram plane reconstructs the first target CIIR image at $z = z_1$. The reconstructed wavefront is considered to be the superposition of spherical waves emitted from each pixel of the hologram plane with diverse phase delays. If Δz is too small, the change in each phase delay term is not enough. Because of the insufficient change in each phase delay, the new wavefront at $z_2 = z_1 + \Delta z$ fails to represent the second target CIIR image without the afterimage of the first one. This is the reason of the existence of the ghost images of the other target images with small depth interval.

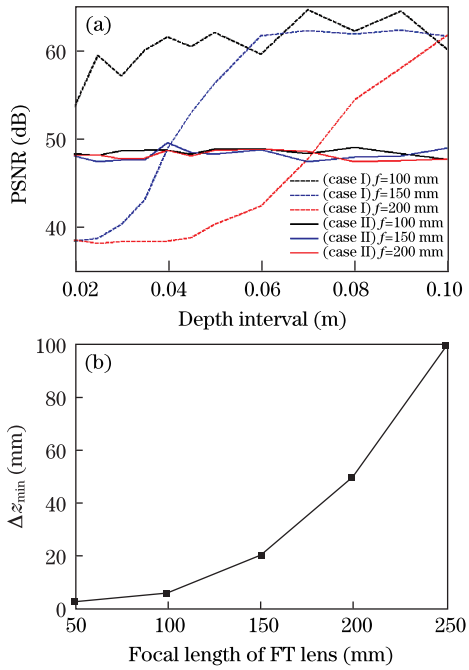

Fig. 5. Simulation results. (a) PSNR values according to the depth interval and (b) minimum representable depth interval with various focal length of the FT lens.

An important factor that determines the minimum depth interval in adjacent depth planes without ghost images, $\Delta z_{\min}$, is the focal length of the FT lens. To verify the relationship between f and $\Delta z_{\min}$, we performed a simulation using a black image with a point light source as the first target image and empty black image as the second target image. If Δz is small, the ghost image of the point source is also shown in the reconstructed second target image. The $\Delta z_{\min}$ is defined as the interval of adjacent planes when the intensity of the ghost image of the point source in the second target image is equal to the half value of the intensity of the original one. In the simulation, f and Δz vary from 50 to 250 mm with the interval of 50 mm, and from 5 to 100 mm with interval of 5 mm, respectively. Figure 5(b) shows the simulation results performed with the two target images of 100 × 100 pixels. This confirms that the FT lens with lower focal length provides smaller $\Delta z_{\min}$ if other parameters remain unchanged. This result coincides with the previous simulation result provided in Fig. 5(a), which verifies that the PSNR value has higher value with lower f.

To suppress the blurred portion of the CIIR images, we estimate the depth of each object based on the optical flow in Ref. [7], and modify the elemental image set for each object. In Ref. [7], the depth extraction and occluded region reconstruction are performed for the orthographic images. However, since the orthographic images have all-in-focus property, they are rearranged and converted into perspective images for generating CIIR images. We assume plane objects for simplicity, and the estimated depth is obtained using the disparity shown in the elemental image set. The original elemental image set can be divided into multiple elemental image sets according to the object's depth by using the appropriate depth threshold. The new elemental image sets contain only the information of one object, and the blurred portion due to the unfocused objects can be eliminated in the modified CIIR images.

However, if the overlapped region between the objects is too large, it is impossible to generate the correct depth-slice images because of the lack of information captured in the elemental image set. In Ref. [7], the authors provided the limitation range in the occluded region that can be reconstructed, which also becomes the limitation region in the modified CIIR method.

We generated CIIR images based on the proposed method with the elemental image set captured in the experimental setup of Fig. 2(a) to verify the effect of suppression for the unfocused objects in our CIIR method. The two elemental image sets are newly generated using the estimated depth map provided in Fig. 2(b), and the CIIR images for each object's depth are generated as shown in Figs. 3(c) and (d). Comparing this with the previous CIIR images, the undesirable part in each CIIR image due to the unfocused object is eliminated.

As discussed previously, the FT lens with low focal length is necessary to display the target images with small depth interval. Instead of using low focal length FT lens, another possible approach to provide small depth interval is to divide the hologram plane and allocate the different holograms of each depth-slice image. The hologram plane is composed of the spatial frequency component of the target images. Therefore, if we divide this spatial frequency domain and assign different holograms, we can represent each hologram respectively.

Unlike in the previous method, each CIIR image in the proposed approach has its own hologram. This means that the N number of phase holograms is generated for representing the N number of CIIR images. The resultant synthesized hologram H_{syn} is composed of multiple sub-holograms for each depth-slice image. If we have two CIIR images and the hologram of the first and second CIIR images are represented as H_1 and H_2, respectively, the division in spatial frequency is demonstrated as

$$H_{\text{syn}}(x,y) = \begin{cases} H_1(x,y), & xy > 0 \\ H_2(x,y), & xy < 0 \end{cases}. \tag{1}$$

In Eq. (1), the position of the (0,0) point is the center of the spatial light modulator (SLM) plane. Figures 4(e) and (f) show the numerically reconstructed results from the hologram provided in Fig. 4(d). The distance between the two target images is the same as those in Figs. 4(b) and (c). However, unlike those in Figs. 4(b) and (c) in which ghost images appear, the reconstructed images in Figs. 4(e) and (f) present desirable target images without ghost images.

The PSNR values according to Δz are provided in Fig. 5(a) for the reconstructed images with the proposed hologram division method. The PSNR values decrease as Δz is decreased without the division in the hologram plane. However, by using hologram division in the proposed method, the PSNR values become almost constant regardless of the decrease in Δz. With the large value of Δz, the PSNR values without hologram division are higher than those with hologram division because there is loss in spatial frequency component in the latter. However, below a certain level of Δz, it is not possible to represent the correct target images for the hologram

without division. The proposed method can provide the individual target image without ghost images.

For the optical reconstruction of the generated hologram, a laser with wavelength of 532 nm is used as a light source and f is 100 mm. We used a phase-only SLM by Holoeye (LC 2002 model), and the maximum resolution is 800 × 600 with pixel pitch of 32 μm. Figure 6 presents the optically reconstructed results with 5 mm of depth interval for the case of undivided and divided hologram, respectively. In Fig. 6(a), the first target image of the object "box" appears with the ghost image of the second target image, which is not reconstructed well. The low figures show that both the first and second target images are reconstructed successfully with the proposed method. Although we did not use the elimination method for the zero-order diffracted light from the SLM, the quality of the optically reconstructed image is enhanced with the use of high-pass filter[11]. We can verify from the experimental results that the CGH using the proposed method can represent the depth-slice images of real objects with small depth interval.

Although the division in the hologram plane shows good results compared with the undivided case, the quality of the image reconstructed from the divided hologram is degraded as the number of division increases. Figure 7 shows the variation of the PSNR values according to

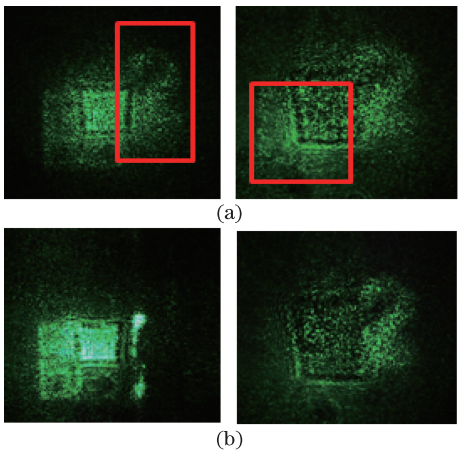

Fig. 6. Optically reconstructed images with 5 mm depth-interval in the case of (a) undivided hologram and (b) divided hologram.

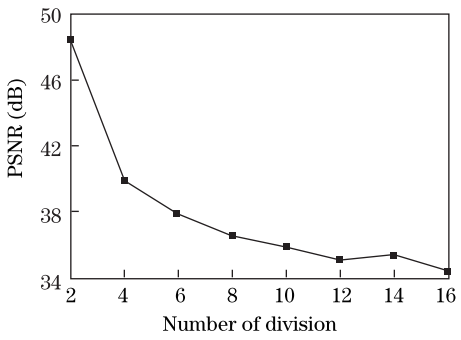

Fig. 7. Variation of PSNR values according to the number of division in the hologram plane.

the number of division, N, in the hologram plane when the depth interval is 5 mm and f is equal to 100 mm. In this simulation, the synthesized hologram is composed of N number of sub-holograms, which satisfy the radial shapes. Since the PSNR value for 5 mm of depth interval and 100 mm of focal length without the hologram division method is around 38 dB, the maximum number of target images allowed is up to six. However, the maximum number of division depends on how the hologram plane is divided, and this can be enhanced if the method for hologram division is optimized.

In conclusion, we introduce a hologram generation method based on II, and propose an enhancement method for depth interval limitation without ghost images. In the CIIR process, the original elemental image set is modified based on the estimated depth of objects to remove the blurred image due to the unfocused object. In addition, we examine the effect of depth interval between adjacent planes on the quality of the reconstructed images. The hologram plane is divided and assigned with the holograms for each depth-slice image to overcome the limitation in depth interval. The principle of the proposed method is verified in the simulation and experiment results, confirming its feasibility. Further research related to the analytical study of representable depth interval and the optimization for hologram plane division will be required.

This work was supported by the Brain Korea 21 Program (Information Technology of Seoul National University).

References

1. P. Benzie, J. Watson, P. Surman, I. Rakkolainen, K. Hopf, H. Urey, V. Sainov, and C. von Kopylow, IEEE Trans. Circ. Syst. Video Technol. **17,** 1647 (2007).
2. T. Mishina, M. Okui, and F. Okano, Appl. Opt. **45,** 4026 (2006).
3. J.-H. Park, M.-S. Kim, G. Baasantseren, and N. Kim, Opt. Express **17,** 6320 (2009).
4. J. Yeom, J. Jong, J.-H. Park, and B. Lee, in *Proceedings of International Workshop on Holographic Memories and Display* 41 (2010).
5. M. Makowski, M. Sypek, A. Kolodziejczyk, G. Mikula, and C. Prokopowicz, Opt. Eng. **44,** 125805 (2005).
6. J.-H. Park, S. Jung, H. Choi, Y. Kim, and B. Lee, Appl. Opt. **43,** 4882 (2004).
7. J.-H. Jung, K. Hong, G. Park, I. Chung, J.-H. Park, and B. Lee, Opt. Express **18,** 26373 (2010).
8. S.-H. Hong, J.-S. Jang, and B. Javidi, Opt. Express **12,** 483 (2004).
9. J.-J. Lee, B.-G. Lee, and H. Yoo, Appl. Opt. **50,** 1889 (2011).
10. J. W. Goodman, *Introduction to Fourier Optics* (3rd ed.) (Roberts & Company Publishers, Greenwood Village, 2004).
11. M. Makowski, I. Ducin, K. Kakarenko, A. Kolodziejczyk, A. Siemion, A. Siemion, J. Suszek, M. Sypek, and D. Wojnowski, Opt. Lett. **36,** 3018 (2011).